The use of different adhesive filling material and mass combinations to restore class II cavities under loading and shrinkage effects: a 3D-FEA

DOI:
10.1080/10255842.2020.1836168

Document Version
Accepted author manuscript

Published in:
Computer Methods in Biomechanics and Biomedical Engineering

The use of different adhesive filling material and mass combinations to restore class II cavities under loading and shrinkage effects: a 3D-FEA

P. Ausiello[1*] , S. Ciaramella[1] , A. De Benedictis[1] , A. Lanzotti[2] , J.P.M. Tribst[3], D.C. Watts[4].

1. Dept. of Neurosciences, Reproductive Sciences and Odotostomatological Sciences, University of Naples, Frederico II, Naples, Italy
2. Department of Industrial Engineering, University of Naples, Frederico II, Naples, Italy
3. Sao Paulo State University (UNESP), São José Campos, Brazil.
4. University of Manchester, School of Medical Sciences and Photon Science Institute, Manchester, UK.

* Corresponding Author

Abstract

Abstract

3D tooth models were virtually restored: flowable composite resin + bulk-fill composite (A), glass ionomer cement + bulk-fill composite (B) or adhesive + bulk-fill composite (C). Polymerization shrinkage and masticatory loads were simulated. All models exhibited the highest stress concentration at the enamel–restoration interfaces. A and C showed similar pattern with lower magnitude in A in comparison to C. B showed lower stress in dentine and C the highest cusps displacement. The use of glass ionomer cement or flowable composite resin in combination with a bulk-fill composite improved the biomechanical behavior of deep class II MO cavities.

Keywords: Adhesion, class II MO, loading, polymerization shrinkage, operative dentistry

Introduction

Resin based dental composites polymeric materials become innovative in restorative dentistry for direct application in dental decay treatment. This restorative material can be applied to aesthetically and functionally rebuild the injured teeth with direct restorations (Sideridou et al. 2011; Yazici et al. 2014; Borgia et al. 2019). Different potential cytotoxic risk effects of dental composites have been described in the past and associated to the resin monomers composition during in vitro tests (Ausiello et al. 2013; Treglia et al. 2012). But there is no clinical evidence reported.

In class I and II dental restorations, when the decay was removed and the final cavity was shaped by the dentist, if it results in a wide deep ranging cavity, different resin based material could be used, as direct (by the dentist) or indirect (by laboratory) techniques. Instruction is required to help dental specialists to make the right decisions according to the options (da Veiga et al. 2016).

Polymer based dental resin composites show a volumetric polymerization shrinkage (post gel shrinkage) from 1% up to 4.5% depending on numerous chemical and physical aspects, specifically the presence of methacrylate matrix monomers and the volume percent of inorganic filler (Davidson and Feilzer 1997).

Polymerization shrinkage and stress are two phenomena hardly linked each other and depending both on the polymer characteristics normally used in dentistry. Young's modulus of the polymer based material (filling, flowable or luting resin composites) associated with cavity geometry (boundary conditions) and stiffness of remaining tissue are considered critical factors in the restoration stress distribution (Al Sunbul et al. 2016).

Shrinkage stresses in adhesively restored class II cavities of posterior teeth act along internal and marginal surfaces and they are potentially able to produce a clinical failure by gap formation (Jantarat et al. 2001; Han et al. 2016). Several investigators justify that stresses in a dental polymer material by the dimensional changes of the material at the interface of tooth or by incidence of the occlusal loads (Versluis et al. 2004).

These phenomena have been investigated both in vitro (Yamada et al. 2004; Braga et al. 2013; Boaro et al. 2014; da Rocha et al. 2019) and in silico simulations (Williams et al. 1987; Kowalczyk 2009; Musani and Prabhakar 2010; Chuang et al. 2011; Rodrigues et al. 2014; Dejak and Młotkowski 2015).

Anyway, clinical success and longevity of dental posterior restorations are related by many factors. These include material selection, patient oral health compliance and the operator's skill (Hickel and Manhart 2001).

Marginal cavity in bonded dentine cavities reflects complex interactions between adhesive bonding, polymerization strain, stress and material elastic modulus (Ausiello et al. 2017a). The level of shrinkage stress and debonding in particular is probably more depending on the shape and hence constrains of the cavity (Correia et al. 2020).

A previous study (Chuang et al. 2011) found that shrinkage of the deepest layer in adhesive class I posterior restorations, where an high C-factor configuration there exist, is directly associated with the material and may result in cervical microleakage (gap) when the stress surpasses the resin–dentine bond strength value. Although the effect of C-factor upon shrinkage stress is clearly demonstrated,

the relationship is more complex than simply a ratio of bonded to unbonded surfaces and that it is also depending on composite material volume involved in the restoration (Watts and Satterthwaite 2008). More, Wang et al., also focused the role of the compliance of the cavity (width deep) in the evaluation of C-factor influence (Wang and Chiang 2016).

In the past, dentists did not restore a 4 mm deep cavity in a single bulk filling. The incremental technique and reduced volume of the first increment of composite were always advised to regulate the shrinkage direction and prevent microleakage (Jang et al. 2015). Today, bulk-fill dental resin composites, may partially overcome some of these limits due to the different chemical monomers composition and translucency (Han et al. 2016; Correia et al. 2020). A literature review (Van Ende et al. 2017) indicated that more clinical studies are still required to fully explore the clinical benefits of bulk-fill composites.

Therefore, the aim of the present investigation was to calculate the mechanical behavior of different restorative materials combinations in restore class II MO cavities by means of a linear elastic 3D finite element analysis (3D-FEA) under the effect of occlusal loading and polymerization shrinkage.

The null hypothesis was there is no different stress distribution on the adhesive interfaces in the various materials combinations used to restore the lost dental volumes.

Materials and Methods

Biomechanical responses in dental applications have been extensively investigated by means of modern CAD–FEM (Computer Aided Design and Finite Element Method) techniques (Martorelli and Ausiello 2013; Braga et al. 2013; da Rocha et al. 2019; Dejak and Młotkowski 2015; Williams et al., 2005; Gloria et al. 2018). Using these techniques, a 3D CAD model of a sound tooth (Figure 1) was created.

Figure 1. 3D CAD model of a sound tooth and three models with class II cavities.

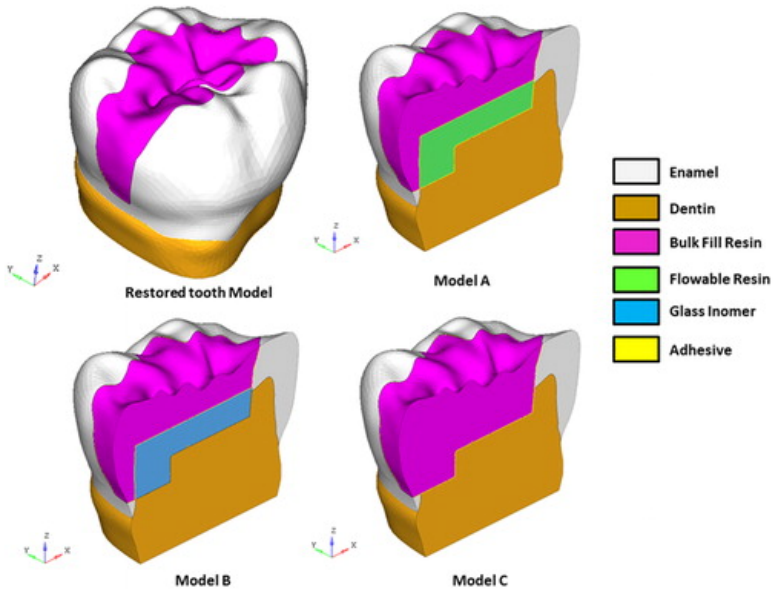

Starting from the 3D CAD model, three models with class II MO (mesio-occlusal) cavities (Figure 1) were obtained to investigate the influence of the restorative materials combinations in replacing different cavities volumes under occlusal loading and polymerization shrinkage.

These models were designated as A, B and C and detailed in Table 1. The geometrical features of models are shown in Figure 1. Different volumes were attributed to the various materials used in the simulation of class II MO restorations.

Table 1. Restorative material combinations and thicknesses

Model	Adhesive layer	Restorative lower layer	Restorative upper layer	Single restorative material
A	10 µm thick	Flowable resin composite (1.5 and 3 mm thick at middle cavity and box respectively, with 35 mm^3 volume)	Bulk fill resin composite (about 2.5 mm thick and 63 mm^3 volume)	–
B	–	Glass-Ionomer cement (GIC) (1.5 and 3 mm thick at middle cavity and box respectively, with 35 mm^3 volume)	Bulk fill resin composite (about 2.5 mm thick and 63 mm^3 volume)	–
C	10 µm thick	–	–	Bulk fill resin composite (about 4 mm at middle cavity and 5.5 mm at the box, with 98 mm^3 volume)

Generation of solid models

A solid sound tooth model was obtained using a reverse engineering technique. The shapes of dentine and enamel were digitized with a high resolution micro-CT scanner system (Bruker micro-CT, Kontich, Belgium). The image data sets were processed *via* InVesalius 3.1.1 software (www.cti.gov.br/en) and 3D tessellated surfaces were created. Starting from 3D tessellated surfaces, cross-section curves were generated and the parametric 3D CAD model was created using loft surfaces in Rhinoceros® (Robert McNeel & Associates, USA). Boolean operations ensured the congruence of interfacial boundaries of dentine and enamel. The tooth model was cut 2.5 mm below the cervical area to obtain the final model (Ausiello et al. 2017b)

The bucco-lingual and mesio-distal widths were 10.60 mm and 12.36 mm, respectively, and the thickness of enamel was of about 1.5 mm. Class II MO lateral internal walls had rounded modelled angles. The tooth model was placed in a coordinate system, with *X* and *Y*-axes for the bucco-lingual and mesio-distal directions, respectively. The *Z*-axis was oriented vertically (Figure 1).

A class II MO cavity, about 4.0 mm deep in the middle and 5.5 mm deep in the box with a bevel of 0.5 mm was shaped all along the enamel class II MO margins was modelled in Rhinoceros® and the restored models were obtained *via* Boolean operations between the cavity, enamel and dentine surfaces.

The variability of the masticatory function, depending on the contact between tooth surface and food bolus, was incorporated by modelling food on the occlusal surface (Figure 2).

Figure 2. Food bolus incorporated by modelling food on the occlusal surface.

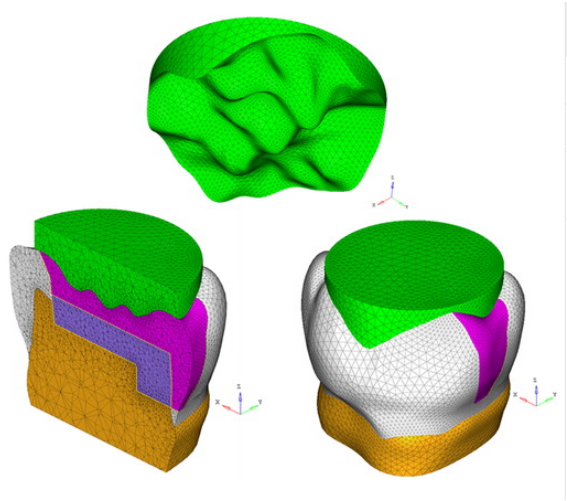

Numerical simulation

The mechanical behavior of three restored models was analyzed *via* three-dimensional FEA using Hyper Works® (Altair Engineering Inc, USA). Three models of a restored tooth with a multilayer construction were created and investigated using different material combinations (Gloria et al. 2018), as summarized in Table 1.

Hyper Works® software was used to mesh components of the models (Giordano et al. 2012). All volumes were discretized by 4-node tetrahedral elements CTETRA with a global size ranging from 0.05 mm to 0.15 mm. To minimize the mesh dependency of results, due to the small radius of curvature and notch effects, mesh refinement techniques were used (Ausiello et al. 2011). The total number of nodes and elements are summarized in Table 2.

Table 2. Analysed tooth models and technical features.

Model	Total number of nodes	Total number of elements	Total number of contact elements	Total of degrees of freedom
A	78,777	360,242	20,311	292,869
B	78,816	354,457	20,310	292,590
C	76,837	352,184	19,050	283,716

Mechanical properties assigned to each material and magnitudes of linear shrinkage (%) of shrinking materials are given in Table 3.

Table 3. Mechanical properties of materials: Young's modulus, Poissons's ratio and linear shrinkage.

Material	Young's modulus (GPa)	Poisson's ratio	Linear shrinkage (%)	References
Dentine	18.0	0.23	-	Ausiello et al. (2017a)
Enamel	80.0	0.30	-	Ausiello et al. (2017a)
Food (apple pulp)	3.41	0.1	-	Ausiello et al. (2019)
Adhesive layer	4.0	0.30	1.0	Ausiello et al. (2019)
Flowable resin composite	8.0	0.25	1.0	Ausiello et al. (2019)
Glass inomer composite (GIC)	8.0	0.25	-	Ausiello et al. (2019)
Bulk fill composite	12.00	0.25	1.0	Ausiello et al. (2017a)

All the FE analyses were focused on load during the closing phase of the chewing cycle (Penteado et al. 2019). The variability of chewing function was considered dependent on the contact between food and tooth surface (Williams et al., 2005). Solid food apple pulp (Williams et al., 2005; Dal Piva et al. 2018) was modelled on the occlusal surface (Figure 2) and slide-type contact elements were used between tooth surface and food.

It is known that shrinkage stresses in teeth restored with composite materials may be less than those calculated on the basis of elastic model. During the curing process, stress relaxation accompanies the viscous flow of composites and the Young modulus *E* and viscosity increase rapidly. To take this into account, the simplified approach proposed by a previous report (Kowalczyk 2009) was used and the final shrinkage smax was reduced according to the rule sr = (sr/s) smax. So, effective linear shrinkage sr = 0.001 was adopted in the analyses. Polymerization shrinkage for the adhesive layers (10 μm uniform thickness) and shrinking materials was simulated with the thermal expansion approach by assigning a one degree drop in temperature (Ausiello et al. 2017a). The adhesive layer, composite resin, enamel and dentine presented ideal interfaces with bonded contacts.

Physiological masticatory loads (Natali et al. 2010) were simulated as an occlusal static load of 600 N and a transversal load of 20 N. These were applied on the food in the vertical and bucco-lingual directions, respectively. These loads were simultaneously applied in combination with shrinkage effects.

Nodal displacements on the lower surfaces of models were constrained in all directions. Static linear analyses were carried out. The simulations were performed considering a non-failure condition and all materials were assumed to behave elastically.

Results

The resultant stress distributions for the models were compared and analyzed. As these materials exhibit brittle behavior, the Maximum Principal Stress was selected to measure the potential damage. Figure 3 shows the first principal stress distributions for enamel, dentine and restorative material for each model due to occlusal loads in combination with shrinkage effect. Two cross sections along the bucco-lingual direction of the restored tooth model were considered, CS1, including the MO middle cavity, and CS2, including the MO cavity box. Figure 4 depicts contour plots of first principal stress for each analyzed model.

Figure 3. First principal stress distributions for enamel, dentine and restorative material for each model due to chewing load in combination with shrinkage effect. Cross sections along the bucco-lingual direction of the tooth were considered.

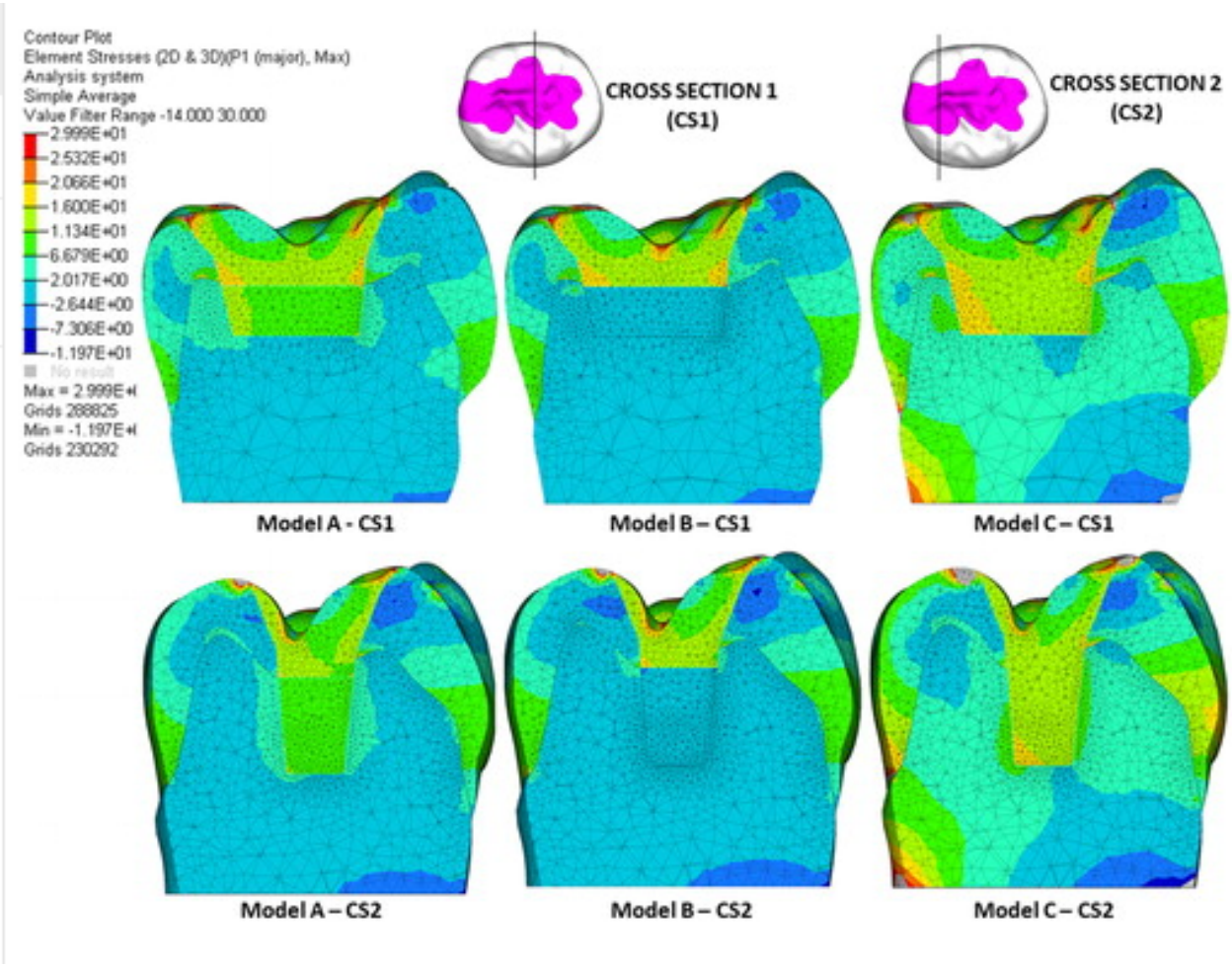

Figure 4. Overall contour plots of First principal stress for each analyzed model.

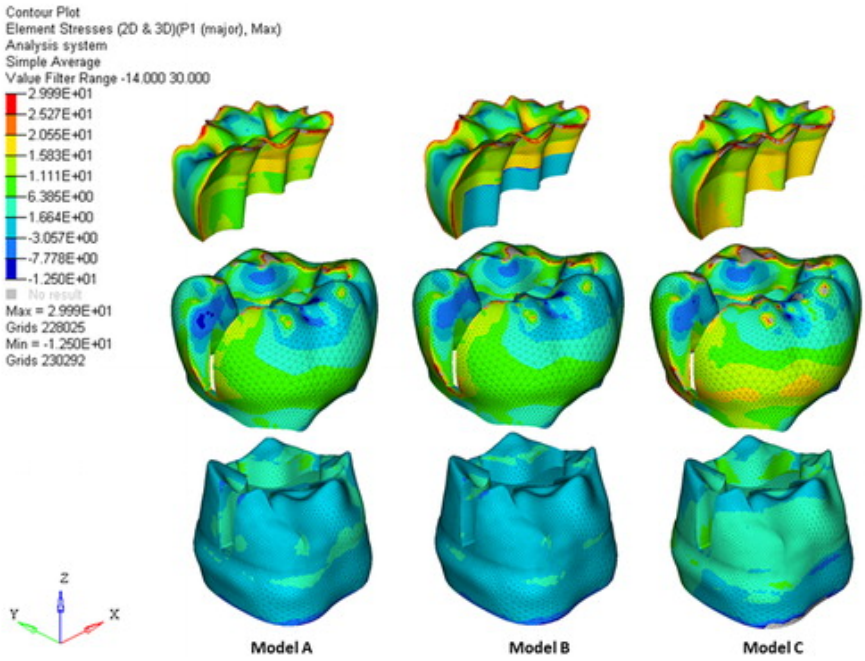

Further quantitative results were observed by inspection line, defined along the cavity wall. For each cross section, first principal stresses were plotted along the inspection line and compared for the different models (Figure 5).

Figure 5. First principal stresses plotted according to the inspection line and compared for the different models near tooth tissues–restoration interfaces. All models showed a similar stress trend along enamel–restoration interface.

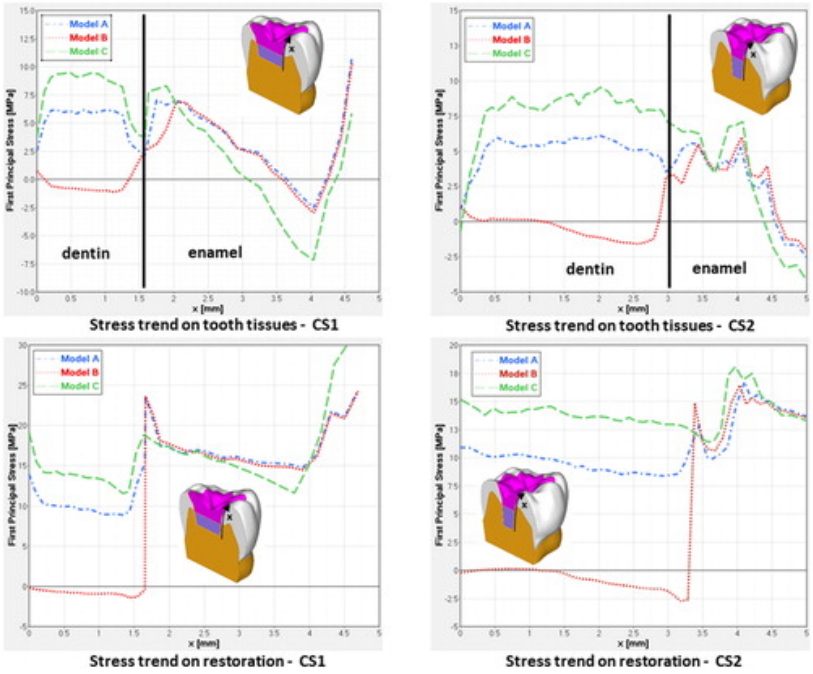

As seen in Figure 3, all the class II MO, A, B and C models exhibited high stress concentration near the occlusal surfaces, in CS1 as well as in CS2. The models showed a similar stress trend along enamel–restoration interfaces, in beveled and not beveled areas (Figure 5, up, left and right).

In the restoration, the highest stress values were located near the edge of the enamel–dentine interface (Figure 3) on the occlusal surface. A and C models (Figure 5) showed a similar stress trend along tooth tissues–restoration interface. A similar stress trend was showed by model B only along enamel–restoration interface, whereas the stress decreases with depth along the dentine–restoration interface and tend to zero at the cavity floor. This occurs for both CS1 and CS2 cross section (Figure 5).

Observing the CS1 in Figure 5, along the dentine–restoration interface stress values of up to 6.0 MPa and 15 MPa were recorded in the dentine and restoration, respectively, for model A, and 9.0 MPa and 19 MPa for model C. In contrast, lower values of up to 2.5 MPa and about zero were recorded in the dentine and restoration, respectively, for model B. For the enamel–restoration interface, the stress values of up to 10 MPa and 24 MPa were recorded in the enamel and restoration, respectively, for both A and B models, while 8.0 MPa and 30 MPa for C model.

Similarly, considering CS2 in Figure 5, along the dentine–restoration interface stress values of up to 6.0 MPa and 12 MPa were recorded in the dentine and restoration, respectively, for model A, 9.0 MPa and 15 MPa for model C and 1.5 MPa and about zero for model B. Along enamel–restoration interface, stress values of up to 6.0 MPa and 17 MPa were recorded in the enamel and restoration, respectively, for both models A and B, 7.5 MPa and 18.5 MPa for model C.

In Figure 4, it is clear the difference for internal stress distribution among model B, where no-shrinking material has been simulated in the deepest 1.5 mm layers, and model C, showed highest stress concentrated in dentine.

Discussion

It has been shown that teeth have complex behavior during chewing function due to anatomical arrangements based on different tissues combinations. Chewing is also influenced by the jaw muscle activity for different foods (Williams et al., 2005). Posterior teeth show a stress distribution depending of shape, rigidity and loading, and even though the mechanical properties of most of the components are well known, it is hard to predict without a complex calculation (Natali et al. 2010).

Enamel presents a high elastic modulus (E = 80 GPa) and dentine is a more compliant one (E = 18 GPa), these combination in posterior teeth allow an increased fracture resistance during mastication and a uniform stress distributions (Williams et al., 2005; Dal Piva et al. 2018).

Several investigations on resin composite adhesive restoration were performed using *in vitro* methods (Burke et al. 1993; Sakaguchi et al. 1997; da Rocha et al. 2019) or using *in silico* simulations (Dejak and Młotkowski 2015; Ausiello et al. 2017a) and have tested the influence of occlusal loading, polymerization shrinkage, cusps deflection, enamel crack propagation and cavities design in the stress distribution.

The knowledge of the stress distribution in restored teeth assist to prevent post restorative problems (Jantarat et al. 2001). The FEA presents advantages over the *in vitro* destructive tests due to it enables the handling of a complex settings and provides a greater insight into detailed results about the internal stress of both tooth and restorations (Ausiello et al. 2017b, 2017c). However, a virtual FEA requires modelling and a complex calculation with correct boundary conditions (Dejak and Młotkowski 2015).

In adhesively restored posterior teeth the materials must create a strong adhesive bridge between the cavity walls (da Rocha et al. 2019) to reproduce the dentine and enamel architecture as closely as possible to the natural teeth (Ausiello et al. 2017a). The purpose is to reduce the debonding, marginal leakage and fracture (Aggarwal et al. 2014). Obviously, morphology, function and aesthetics must also be replicated.

In the present investigation, the mechanical response in three models with class II MO (mesioocclusal) restorations has been simulated. The more adverse outcomes were found in models C and A. Figures 3 and 4 show the highest stresses concentration at the cavity margin. For these models, an adhesive (E = 4GPa) and bulk-fill composite (E = 12 GPa) or a combination of adhesive (E = 4 GPa) with a flowable composite (E = 8 GPa) and a bulk filling composite (E = 12 GPa) were used.

Resin composite thickness and its Young's modulus strongly influence the stress concentration at adhesive interfaces particularly in terms of cusps displacement (Jantarat et al. 2001; da Rocha et al. 2019). The present investigation confirmed that in class II cavities the no-shrinking material combination can improve the mechanical behavior of the restorations (Ausiello et al. 2017c).

For model C, the highest stress concentration at tooth tissues and restorations interfaces (which has been considered as a measure of failure probability) was calculated and also the higher value of

cusps displacement in the cervical area of the tooth as shown in Figure 3. These findings have been partially shown in large class II MOD adhesive restorations (Ausiello et al. 2017c).

The stress results were probably not dependent on the C-factor configuration but also upon the restorative material linearly polymerization shrinkage (Watts and Satterthwaite 2008) and Young's modulus.

In particular, models A and C, with cavity volume of 98 mm^3, showed a different susceptibility to damage, with highest stress levels in the cavity zone that involve the dentine. Furthermore, model A, restored with a more flexible material (8 GPa) mass to fill a 63 mm^3 of dental volume showed (in combination with a bulk-fill composite, E = 12GPa, volume of 35 mm^3) a lower stress level in comparison with model C where a stiffer composite mass (12 GPa) was simulated to fill a single layer a dental cavity volume of 98 mm^3.

Model B, with a 1% shrinking bulk-fill composite mass (E = 12 GPa) in restoring a volume of 35 mm^3 in combination with a no-shrinking deeper layer (E = 8 GPa, volume of 63 mm^3), showed a decreases stress trend near zero at the cavity floor (Figures 3-5). The results (Figures 4 and 5) suggest that this combination has distinctly more consequences than occlusal loading as previously suggested (Oliveira Schliebe et al. 2016).

This found partially limit the role of the C-factor in the stress generated at the class II restorations interfaces but correlate the stresses to the cavity compliance (Wang and Chiang 2016). In the past, it was described that an adhesive interface was able to reduce the stresses from shrinkage and loading in adhesive class II (Versluis et al. 2004). A possible explanation for this behavior can be attributed to the ratio thickness/E modulus of the restorative materials.

Observing CS1 as well as CS2 indicates that the new generation of conventional and bulk-fill composites had not reduced shrinkage stress compared to bulk-flow composites (Oliveira Schliebe et al. 2016). In this context, shrinkage stress has evidently greater influence than occlusal loading. Kim et al. (2015) concluded that despite the benefits of the bulk-fill composites, clinicians should not entirely replace the conventional composites but combine their use when deep cavities are considered.

Both the configuration factor and the type of bulk-fill composite have a great impact on bonding to cavity restorations (Van Ende et al. 2013, 2016). These findings confirm that mathematical analyses must be considered to study restoration C-factor and translate it to clinical recommendations (Watts and Satterthwaite 2008).

Looking at model B, with a non-shrinking GIC lower filling mass, it is evident that it produced the lowest stress concentration effect (compared to models A and C) with a reduced cusp displacement. It is evident that many factors are involved in the full explanation of polymerization internal and marginal shrinkage stresses, cusp displacement and marginal failure risk in class I and II restorations (Davidson and Feilzer 1997; da Rocha et al. 2019).

A previous report (Kowalczyk 2009) confirmed the need of the resin based composite layering technique to reduce the polymerization stresses in large cavities. These findings support our results considering the influence of the restorative material stiffness and layering to restore different volumes of the lost dental tissues. This statement is in accord with a previous investigation (Aggarwal et al. 2014) that suggested a possible advantage of a liner material to reduce leakage in class II restorations. In this case, the use of glass ionomer materials should be considered (Aggarwal et al. 2014; Ausiello et al. 2019; Han and Park 2018).

Oglakci et al. (2019) recently found *in vitro* by X-ray microcomputed tomography the use of a GIC as liner produced a significant reduction in gap formation when used in combination with bulk fill high viscosity composites.

Politi et al. (2018) suggested alternative tools to reduce cuspal displacement and microleakage score in adhesively restored molar teeth. The use of different restorative protocols of resin based composite restoratives (conventional and bulk fill) 'significantly improved bond integrity and could be translated as a validation of the limited clinical studies available on bulk-fill materials in the dental literature where Class II cavities perform less well than Class I cavities following extended follow-up'.

Other factors such as light irradiation sources (Apicella et al. 2002; Schneider et al. 2012; Zarone et al. 2019) can influence resin composite polymerization shrinkage stress and resin monomers degree of conversion. It would appear that light irradiation of individual conventional resin based composites or bulk-fill resin restoratives may be problematic such that material selection is vital in the absence of clinical data (McHugh et al. 2017). However, the null hypothesis of the present investigation was rejected.

This FEA, assuming isotropic elastic material materials behavior, suggests the following:

Models A and C (posterior teeth with class II MO deep cavities) showed a different susceptibility to damage, with the highest stress levels in the cavity zone in model C;

Lower stress values were detected in model A when a flowable composite restorative material was applied to restore the deepest 65 mm^3 of the dental cavity in combination with a bulk-fill composite;

Model B showed a promising mechanical response when a non-shrinking restorative material was applied as the deepest restorative layer in combination with a limited bulk-fill composite mass to fill 33 mm^3 of the dental cavity.

Disclosure Statement

No potential conflict of interest was reported by the authors.

References

1. Aggarwal V, Singla M, Yadav S, Yadav H. 2014. Effect of flowable composite liner and glass ionomer liner on class II gingival marginal adaptation of direct composite restorations with different bonding strategies. J Dent. 42(5):619–625.
2. Al Sunbul H, Silikas N, Watts DC. 2016. Polymerization shrinkage kinetics and shrinkage–stress in dental resin-composites. Dent Mater. 32(8):998–1006.
3. Apicella A, Di Palma L, Aversa R, Ausiello P. 2002. DSC kinetic characterization of dental composites using different light sources. J Adv Mater. 34(4):22–25.
4. Ausiello P, Cassese A, Miele C, Beguinot F, Garcia-Godoy F, Di Jeso B, Ulianich L. 2013. Cytotoxicity of dental resin composites: an in vitro evaluation. J Appl Toxicol. 33(6):451–457
5. Ausiello P, Ciaramella S, Garcia-Godoy F, Martorelli M, Sorrentino R, Gloria A. 2017a. Stress distribution of bulk-fill resin composite in class II restorations. Am J Dent. 30(4):227–232.

6. Ausiello P, Ciaramella S, Martorelli M, Lanzotti A, Gloria A, Watts DC. 2017c. CAD-FE modeling and analysis of class II restorations incorporating resincomposite, glass ionomer and glass ceramic materials. Dent Mater. 33(12):1456–1465.
7. Ausiello P, Ciaramella S, Martorelli M, Lanzotti A, Zarone F, Watts DC, Gloria A. 2017b. Mechanical behavior of endodontically restored canine teeth: effects of ferrule, post material and shape. Dent Mater. 33(12):1466–1472.
8. Ausiello P, Franciosa P, Martorelli M, Watts DC. 2011. Numerical fatigue 3D-FE modeling of indirect composite-restored posterior teeth. Dent Mater. 27(5):423–430.
9. Ausiello P, Ciaramella S, Lanzotti A, Ventre M, Borges AL, Tribst JP, Dal Piva A, Garcia-Godoy F. 2019. Mechanical behavior of Class I cavities restored by different material combinations under loading and polymerization shrinkage stress. A 3D-FEA study. Am J Dent. 32(2):55–60.
10. Boaro LC, Brandt WC, Meira JB, Rodrigues FP, Palin WM, Braga RR. 2014. Experimental and FE displacement and polymerization stress of bonded restorations as a function of the C-factor, volume and substrate stiffness. J Dent. 42(2):140–148.
11. Borgia E, Baron R, Borgia JL. 2019. Quality and survival of direct light-activated composite resin restorations in posterior teeth: a 5 to 20 year retrospective longitudinal study. J Prosthodont. 28(1):195–203.
12. Braga RR, Koplin C, Yamamoto T, Tyler K, Ferracane JL, Swain MV. 2013. Composite polymerization stress as a function of specimen configuration assessed by crack analysis and finite element analysis. Dent Mater. 29(10):1026–1033.
13. Burke FJ, Wilson NH, Watts DC. 1993. The effect of cavity wall taper on fracture resistance of teeth restored with resin composite inlays. Oper Dent. 18(6):230–236.
14. Chuang SF, Chang CH, Chen TY. 2011. Contraction behaviors of dental composite restorations-finite element investigation with DIC validation. J Mech Behav Biomed Mater. 4(8):2138–2149.
15. Correia A, Andrade MR, Tribst J, Borges A, Caneppele T. 2020. Influence of bulk-fill restoration on polymerization shrinkage stress and marginal gap formation in class V restorations. Oper Dent. 45(4):E207–E216.
16. da Rocha DM, Tribst JPM, Ausiello P, Dal Piva AMDO, da Rocha MC, Di Nicoló R, Borges ALS. 2019. Effect of the restorative technique on load-bearing capacity, cusp deflection, and stress distribution of endodontically-treated premolars with MOD restoration. Restor Dent Endod. 44(3):e33.
17. da Veiga AMA, Cunha AC, Ferreira DMTP, da Silva Fidalgo TK, Chianca TK, Reis KR, Maia LC. 2016. Longevity of direct and indirect resin composite restorations in permanent posterior teeth: a systematic review and meta-analysis. J Dent. 54:1–12.
18. Dal Piva AMO, Tribst JPM, Borges ALS, Souza ROAE, Bottino MA. 2018. CAD-FEA modeling and analysis of different full crown monolithic restorations. Dent Mater. 34(9):1342–1350.
19. Davidson CL, Feilzer AJ. 1997. Polymerization shrinkage and polymerization shrinkage stress in polymerbased restoratives. J Dent. 25(6):435–440.
20. Dejak B, Młotkowski A. 2015. A comparison of stresses in molar teeth restored with inlays and direct restorations, including polymerization shrinkage of composite resin and tooth loading during mastication. Dent Mater. 31(3):77–87.
21. Giordano M, Ausiello P, Martorelli M. 2012. Accuracy evaluation of surgical guides in implant dentistry by noncontact reverse engineering techniques. Dent Mater. 28(9):178–185.
22. Gloria A, Maietta S, Martorelli M, Lanzotti A, Watts DC, Ausiello P. 2018. FE analysis of conceptual hybrid composite endodontic post designs in anterior teeth. Dent Mater. 34(7):1063–1071.

23. Han SH, Sadr A, Tagami J, Park SH. 2016. Internal adaptation of resin composites at two configurations: influence of polymerization shrinkage and stress. Dent Mater. 32(9):1085–1094.
24. HanSH, ParkSH. 2018. Incremental and bulk-fill techniques with bulk-fill resin composite in different cavity configurations. Oper Dent. 43(6):631–641.
25. Hickel R, Manhart J. 2001. Longevity of restorations in posterior teeth and reasons for failure. J Adhes Dent. 3(1):45–64.
26. Jang JH, Park SH, Hwang IN. 2015. Polymerization shrinkage and depth of cure of bulk-fill resin composites and highly filled flowable resin. Oper Dent. 40(2):172–180.
27. Jantarat J, Palamara JE, Messer HH. 2001. An investigation of cuspal deformation and delayed recovery after occlusal loading. J Dent. 29(5):363–370.
28. Kim RJ, Kim YJ, Choi NS, LeeI B. 2015. Polymerization shrinkage, modulus, and shrinkage stress related to tooth-restoration interfacial debonding in bulk-fill composites. J Dent. 43(4):430–439.
29. Kowalczyk P. 2009. Influence of the shape of the layers in photocured dental restorations on the shrinkage stress peaks-FEM study. Dent Mater. 25(12):83–91.
30. Martorelli M, Ausiello P. 2013. A novel approach for a complete 3D tooth reconstruction using only 3D crown data International. Int J Interact Des Manuf. 7(2):125–133.
31. McHugh LEJ, Politi I, AlFodeh RS, Fleming GJP. 2017. Implications of resin-based composite (RBC) restoration on cuspal deflection and microleakage score in molar teeth: placement protocol and restorative material. Dent Mater. 33(9):329–335.
32. Musani I, Prabhakar AR. 2010. Biomechanical stress analysis of mandibular first permanent molar; restored with amalgam and composite resin: a computerized finite element study. Int J Clin Pediatr Dent. 3(1):5–14.
33. Natali AN, Carniel EL, Pavan PG. 2010. Modelling of mandible bone properties in the numerical analysis of oral implant biomechanics. Comput Methods Programs Biomed. 100(2):158–165.
34. Oglakci B, Kazak M, Donmez N, Dalkilic EE, Koymen SS. 2019. The use of a liner under different bulk-fill resin composites: 3D GAP formation analysis by X-ray microcomputed tomography. J Appl Oral Sci. 28:e20190042.
35. Oliveira Schliebe LRS, Lourenço Braga SS, da Silva Pereira RA, Bicalho AA, Veríssimo C, Novais VR, VersluisA, Soares CJ. 2016. The new generation of conventional and bulk-fill composites do not reduce the shrinkage stress in endodontically treated molars. Am J Dent. 29(6):333–338.
36. Penteado MM, Tribst JPM, Dal Piva AM, Ausiello P, Zarone F, Garcia-Godoy F, Borges AL. 2019. Mechanical behavior of conceptual posterior dental crowns with functional elasticity gradient. Am J Dent. 32(4):165–168.
37. Politi I, McHugh LEJ, Al-Fodeh RS, Fleming GJP. 2018. Modification of the restoration protocol for resin-based composite (RBC) restoratives (conventional and bulk fill) on cuspal movement and microleakage score in molar teeth. Dent Mater. 34(9):1271–1277.
38. Rodrigues FP, Lima RG, Muench A, Watts DC, Ballester RY. 2014. A method for calculating the compliance of bonded-interfaces under shrinkage: validation for Class I cavities. Dent Mater. 30(8):936–944.
39. Sakaguchi RL, Versluis A, Douglas WH. 1997. Analysis of strain gage method for measurement of postgel shrinkage in resin composites. Dent Mater. 13(4):233–239.
40. Schneider LF, Cavalcante LM, Prahl SA, Pfeifer CS, Ferracane JL. 2012. Curing efficiency of dental resin composites formulated with camphorquinone or trimethylbenzoyldiphenylphosphine oxide. Dent Mater. 28(4):392–397.
41. Sideridou ID, Karabela MM, Vouvoudi ECh. 2011. Physical properties of current dental nanohybrid and nanofill light-cured resin composites. Dent Mater. 27(6):598–607.

42. Treglia AS, Turco S, Ulianich L, Ausiello P, Lofrumento DD, Nicolardi G, MieleC, Garbi C, Beguinot F, Di Jeso B. 2012. Cell fate following ER stress: just a matter of "quo ante" recovery or death? Histol Histopathol. 27(1):1–12.
43. Van Ende A, De Munck J, Lise DP, Van MeerbeekB . 2017. Bulk-fill composites: a review of the current literature. J Adhes Dent. 19(2):95–109.
44. Van Ende A, De Munck J, Van Landuyt K, Van Meerbeek B. 2016. Effect of bulk-filling on the bonding efficacy in occlusal class I cavities. J Adhes Dent. 18(2):119–124
45. Van Ende A, De Munck J, Van Landuyt KL, Peumans M, Van Meerbeek B. 2013. Bulk-filling of high C factor posterior cavities: effect on adhesion to cavity bottom dentin. Dent Mater. 29(3):269–277.
46. Versluis A, Tantbirojn D, Pintado MR, DeLong R, Douglas WH. 2004. Residual shrinkage stress distributions in molars after composite restoration. Dent Mater. 20(6):554–564.
47. Wang Z, Chiang MY. 2016. Correlation between polymerization shrinkage stress and C-factor depends upon cavity compliance. Dent Mater. 32(3):343–352.
48. Watts DC, Satterthwaite JD. 2008. Axial shrinkage-stress depends upon both C-factor and composite mass . Dent Mater. 24(1):1–8.
49. Williams KR, Edmundson JT, Rees JS. 1987. Finite element stress analysis of restored teeth. Dent Mater. 3(4):200–206.
50. Williams SH, Wright BW, Truong V, Daubert CR, Vinyard CJ. 2005. Mechanical properties of foods used in experimental studies of primate masticatory function. Am J Primatol. 67(3):329–346.
51. Yamada Y, Tsubota Y, Fukushima S. 2004. Effect of restoration method on fracture resistance of endodontically treated maxillary premolars. Int J Prosthodont. 17(1):94–98.
52. Yazici AR, Ustunkol I, Ozgunaltay G, Dayangac B. 2014. Three-year clinical evaluation of different restorative resins in class I restorations. Oper Dent. 39(3):248–255
53. Zarone F, Di Mauro MI, Ausiello P, Ruggiero G, SorrentinoR. 2019. Current status on lithium disilicate and zirconia: a narrative review. BMC Oral Health. 19(1):134.
54.